Crawley, UK). Quantitative PCR (qPCR) and quantitative nested PCR (nPCR) detection for HTLV-1 were performed as described previously.[11–13] Briefly, primers were set in the pX region, and the density of the template was 30 ng per reaction. The PVL was normalized using β-globin and represented as a percentage. The detection density level was in a linear range of ~0.5% and the lowest sensitivity was 0.1%. Furthermore, when presenting 0.1% or less, we conducted nPCR[14] and sub-classified these samples into two types of qPCR (−) and nPCR (+), and both were negative in un-infected cases.

Statistics

To evaluate the test and diagnostic performance for the qualitative detection of anti-HTLV-1, Cohen's kappa-statistics were used. This is a more robust measure than a simple % agreement calculation.

RESULTS

Various Results with the Four Methods

The positive rates by PA, CLEIA, CLIA, and WB were significantly different between the former three methods and WB (Table 1) using pregnant blood samples. The cause of the low positive rate in WB was likely high indeterminates (14.3%). The band patterns of WB and serological and molecular status for HTLV-1 positivity are compared in Table 2. The 15 indeterminate samples consisted of 6 with no only gp46 band pattern (group A) and 9 with no gp46 and gag band (p53, p24 or p19) pattern (group B). Samples of Group A were seropositive in all but case no 21. In addition, all 3 samples (case no. 62, 60, and 100) available for molecular testing showed either a qPCR or nPCR positive reaction (Figure 1). When no amplicon was observed, the sample was re-evaluated using an increased dose of template (60 ng). The amplicon curve in case 62 of Figure 1a emerged as a consequence of an

TABLE 1 The HTLV-1 Serological Results of 105 Pregnant Sera by Each Method

	PA	CLEIA	CLIA	WB (WHO)
Positive	99 (94.3%)	98 (93.3%)	97 (92.4%)	86 (81.9%)
Indeterminate	0	0	0	15 (14.3%)
Negative	6 (5.7%)	7 (6.7%)	8 (7.6%)	4 (3.89%)

The positive rate was significantly lower in WB compared to other 3 methods (<.05) with high indeterminates in 15 sera.

TABLE 2 Comparison of Results between Three Sets of Serological Data for the CLEIA, CLIA and PA; and 19 Cases Showing Four Negative and 15 Indeterminate WB

							Band Pattern gag			Molecular Test	
	Case No.	CLEIA	CLIA	PA	WB Results	env gp46	p53	p24	P19	qPCR	nPCR
group A	21	0.5	0.12	+	Indeterminate	−	+	+	+		
	60	25.9	44.15	+	Indeterminate	−	+	+	+	0.01% (+)	(+)
	50	14.3	90.7	+	Indeterminate	−	+	+	+		
	35	2.4	3.98	+	Indeterminate	−	+	+	+		
	100	8.3	53.12	+	Indeterminate	−	+	+	+	0.02% (+)	(+)
	3	34	90.4	+	Indeterminate	−	+	+	+		
group B	92	0.2	0.14	−	Indeterminate	−	−	+	−		
	64	0.1	0.27	−	Indeterminate	−	−	+	−		
	18	6.3	53.44	+	Indeterminate	−	−	+	−		
	58	0.1	0.13	−	Indeterminate	−	−	−	+		
	32	1.7	1.54	+	Indeterminate	−	−	−	+		
	65	1.2	7.55	−	Indeterminate	−	−	−	+		
	62	14.7	40.17	+	Indeterminate	−	−	−	+	(+)	(+)
	15	5.5	4.95	+	Indeterminate	−	+	−	+		
	33	8.7	24.45	+	Indeterminate	−	+	−	+		
group C	29	3.3	0.1	−	−	−	−	−	−		
	67	0.1	0.12	−	−	−	−	−	−		
	94	0.2	0.12	−	−	−	−	−	−		
	40	0.1	0.49	+	−	−	−	−	−		

The cut of value for CLEIA and CLIA is 1.0. qPCR and nested PCR gave a positive amplicon in all cases tested.

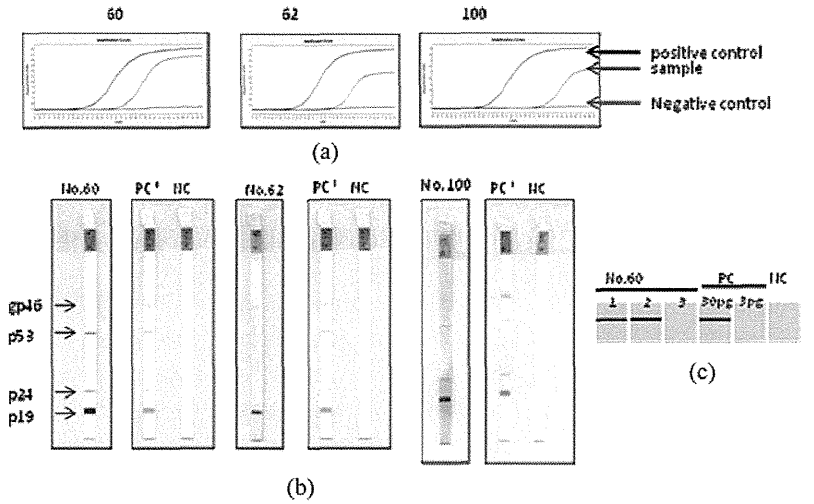

FIGURE 1 (a) Amplicon curve in Real-time qPCR in 3 samples with indeterminate WB pattern. The amplicon curve incompletely elevated out of the dynamic range using 100 ng templates. (b) Western blot pattern of three sampled and that were not observed gp 46 band, where PC* is weak positive control. In order to determine sero-positive, both gp46 and one or more gag band (p53, p24, or p19) were positive. (c) The results of triplicate nested PCR in case no. 60 were showed three images in left panel. PCR was two times positive amplification reaction detecting agarose gel analysis, where PC means positive control and NC means negative control. PC has two different concentrations 30 pg and 3 pg (color figure available online).

TABLE 3 The Proportional Agreement and Kappa-Statistic between the Two Methods

	Proportion of Agreement	Kappa-Statistics
PA-WB	0.88	0.488
CLEIA-WB	0.87	0.428
CLIA-WB	0.89	0.542
PA-CLEIA	0.96	0.693
PA-CLIA	0.96	0.846
CLEIA-CLIA	0.99	0.928

The values of kappa-statistics were evaluated to be poor in less than 0.4, moderate in 0.4–0.59, good in 0.6–0.79, and excellent in 0.89–1.0.

increased template dose. These findings indicate that most samples with indeterminate WB patterns contain a very small number of HTLV-1 provirus-integrated cells (Table 2). Thus, the condition of gp46 positivity in the WHO criteria may not be ideal.

The value of kappa-statistics concerning the validation of test performance in a combination of the two methods is summarized in Table 3. The two chemi-luminescent immune assays (CLEIA and CLIA) kits were evaluated to be excellent.

The Role of PCR in the Serological Diagnostic Strategy of HTLV-1 Infection

About half the cases with sero-indeterminate WB patterns had negative or low titers in other assays. Accordingly, we examined whether the HTLV-1 provirus could be detected in low titer samples or sero-negative converted samples selected from 350 ATL patients who underwent bone marrow transplantation (BMT) and/or chemotherapy. As shown in Table 4, PVL was 0 to 0.5% in 25 of the 350 samples, consisting of 14 sero and molecular positive samples (group I), 7 negative qPCR samples with or without sero-positivity (group II), and 4 sero-negative and qPCR (−) nPCR (+) or (−) samples (group III). This means that serological detection of HTLV-1 infection is better than qPCR for blood samples with a PVL of less than around 0.4%. However, if the detection sensitivity of qPCR was supplemented with nPCR, such molecular methods gave high detection rates. No sample was nPCR (−) and sero-positive. The value of kappa-statistics in the combination of qPCR and CLEIA was 0.545 and the combination of qPCR or nPCR and CLEIA was 0.744, respectively. These findings indicate we should use qPCR or nPCR and CLEIA when we test unnatural samples collected in the complete remission state after BMT and/or chemotherapy in patients with ATL. The discrepancy between the provirus by qPCR and anti-body by CLEIA seems to be related to the detection sensitivity.

TABLE 4 Comparison of the Serological and Proviral Status in Hospitalized Patients with ATL Treated by Either BMT or Intensive Chemotherapy

		Case No	PVL (%)	nestedPCR	Amplified Site of Standard Curve	CLEIA
group I	qPCR (+)	1	0.50%	NT	border	1.3
		2	0.50%	NT	out of linear R	14.9
		3	0.50%	NT	out of linear R	10.5
		4	0.50%	NT	out of linear R	2.4
		5	0.40%	NT	out of linear R	38.1
		6	0.40%	NT	out of linear R	38.1
		7	0.40%	NT	out of linear R	over 1.0
		8	0.40%	NT	out of linear R	over 1.0
		9	0.40%	NT	out of linear R	2.4
		10	0.40%	NT	out of linear R	over 1.0
		11	0.40%	NT	out of linear R	over 1.0
		12	0.40%	NT	out of linear R	2.4
		13	0.40%	NT	out of linear R	39.5
		14	0.40%	NT	out of linear R	14.3
group II	qPCR (−)	15	0.00%	nPCR (+)	no amplicon curve	1.2
	nPCR (+)	16	0.00%	nPCR (+)	no amplicon curve	5.4
		17	0.00%	nPCR (+)	no amplicon curve	6.3
		18	0.00%	nPCR (+)	no amplicon curve	9.8
		19	0.00%	nPCR (+)	no amplicon curve	18.9
	qPCR (−)	20	0.00%	nPCR (+)	no amplicon curve	0.1
	nPCR (+)	21	0.00%	nPCR (+)	no amplicon curve	0.9
group III	qPCR (−)	22	0.00%	nPCR (−)	no amplicon curve	0.5
	nPCR (−)	23	0.00%	nPCR (−)	no amplicon curve	0.8
		24	0.00%	nPCR (−)	no amplicon curve	0.8
		25	0.00%	nPCR (−)	no amplicon curve	0.2

The cut off value of CLEIA is 1.0. (+): positive, but no number data.
NT = not tested.

DISCUSSION

Since the discovery that HTLV-1 is causative for ATL as well as HAM/TSP,[15,16] about 30 years have passed. However, the number of HTLV-1 carriers and annual morbidity number of ATL patients are about 1 million and about 1,000 respectively in Japan.[17] Furthermore, there has been little advance in the treatment for ATL. If people are not infected with HTLV-1, no ATL develops, indicating that prevention of HTLV-1 transmission is important. The natural transmission route is known mainly to be mother to child via breastfeeding.[18–21] The preventive effect of refraining from breast-milk has been demonstrated through the ATL Prevention Program in Nagasaki (APP), which started in 1986.[18,22] On the other hand, a nationwide prevention program similar to APP only started in Japan from 2011, including non endemic areas for HTLV-1. The low prevalence of infection leads to a greater frequency of indeterminate or false positive results. In general, PA and CLEIA (or CLIA) methods are applied as the screening test. If HTLV-1 is positive, the result is confirmed by WB, as

a confirmatory test. Therefore, the final indeterminate judgment may be undesirable for mental health of the mother. In fact, this strategy yields a high rate of inconclusive or equivalent results. Accordingly, it is now controversial as to whether or not real-time qPCR can be substituted for WB.

The present article reveals that although the positive rates of PA, CLEIA, and CLIA were equally high, the values of kappa-statistics gave a more robust evaluation in terms of test performance. Both CLEIA and CLIA showed high proportional agreement, while WB was the worst performer; no validity as a confirmatory test was found. The reason for this appears to result be presence of many sero-indeterminates (14.3%) in endemic erea (Nagasaki). Additionally, the present study indicated that 60–70% of WB indeterminates were probably positive, in particular in cases with no gp46 band. Taken together, the CLEIA (and/or CLIA) is probably suitable for the first screening, but there seems to be no appropriate serological test as a confirmatory test.

Moreover, when serological assays yield discrepant results, no one knows which result is correct. From biological and confirmatory points of view, the genetic approach is promising and attractive. Thus, we compared test and diagnostic performance of PCR and serological assays. Although the benefits of real-time qPCR are well understood, as summarized schematically in Figure 2, the detection limit of 0.01% is a disadvantage of this technology. However, since a combination with nPCR became sensitive at 0.001%, nPCR (−) may be thought of as un-infected. Currently, the pathological significance in

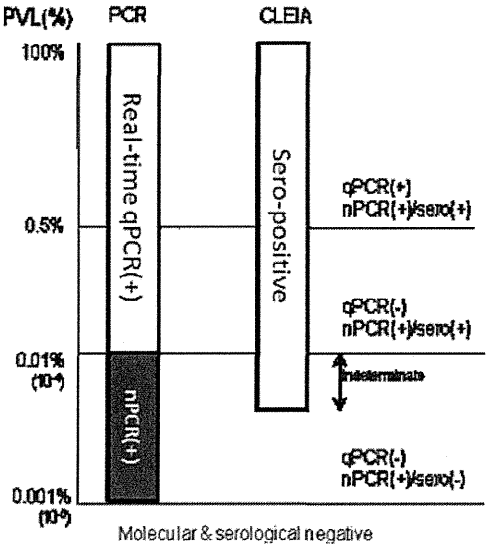

FIGURE 2 The relationship between the HTLV-1 molecular proviral detection status by PCR methodology and the HTLV-1 sero-positive status measured with the CLEIA method.

such a very low number of infected cells remains to be elucidated. In general, the limit of detection of qPCR is thought to be 0.01–0.5%.[13,23–27] the same as with our method. If we convert 0.01% of PVL into total infected cells per body, a total of $3 \times 10^{-4\sim-5}$ infected cells exist within the whole body, indicating that such an infected cell burden seems to be natural in the production of anti-HTLV-1 antibodies. Since even some samples with qPCR (−) and nPCR(+) were positive for the antibody, real-time qPCR may yield seropositive individuals carrying a small number of infected cells detected by only nPCR. This suggests that a combination of qPCR and nPCR is a better algorithm as a confirmatory test.

In conclusion, the high values of kappa-statistics are expected to deliver high quality in CLEIA (or CLIA), while the problems with WB assays remain to be elucidated. As an alternative to WB, a combination of real-time qPCR and nested PCR is proposed as a suitable confirmatory test.

ACKNOWLEDGMENTS

The authors thank staff members in all collaborating institutions and other technical members in the central office of the ATL Prevention Program Nagasaki for efforts in sample collecting and testing.

REFERENCES

1. Miyoshi, I.; Kubonishi, I.; Sumida, M.; Hiraki, S.; Tsubota, T.; Kimura, I.; Miyamoto, K.; Sato, J. A Novel T-cell Line Derived from Adult T-cell Leukemia. *Gann* **1980**, *71*, 155–156.
2. Yoshida, M.; Miyoshi, I.; Hinuma, Y. Isolation and Characterization of Retrovirus from Cell Lines of Human Adult T-cell Leukemia and its Implication in the Diseases. *Proc. Natl. Acad. Sci. USA* **1982**, *79*, 2031–2035.
3. Hinuma, Y.; Nagata, K.; Hanaoka, M.; Nakai, M.; Matsumoto, T.; Kinoshita, K. I.; Shirakawa, S.; Miyoshi, I. Adult T-cell Leukemia: Antigen in an ATL Cell Line and Detection of Antibodies to the Antigen in Human Sera. *Proc. Natl. Acad. Sci. USA* **1981**, *78*, 6476–6480.
4. Poiesz, B. J.; Ruscetti, F. W.; Gazdar, A. F.; Bunn, P. A.; Minna, J. D.; Gallo, R. C. Detection and Isolation of Type C Retrovirus Particles from Fresh and Cultured Lymphocytes of a Patient with Cutaneous T-cell Lymphoma. *Proc. Natl. Acad. Sci. USA* **1980**, *77*(12), 7415–7419.
5. Fujino, R.; Kawato, K.; Ikeda, M.; Miyakoshi, H.; Mizukoshi, M.; Imai, J. Improvement of Gelatin Particle Agglutination Test for Detection of Anti-HTLV-I Antibody. *Jpn. J. Cancer Res.* **1991**, *82*, 367–370.
6. Fujiyama, C.; Fujiyoshi, T.; Matsumoto, D.; Tamashiro, H.; Sonoda, S. Evaluation of Commercial HTLV-1 Test Kits by a Standard HTLV-1 Serum Panel. *Bull. WHO* **1995**, *73*, 515–521.
7. Taguchi, H.; Sawada, T.; Fujishita, M.; Morimoto, T.; Niiya, K.; Miyoshim, I. Enzyme-linked Immunosorbent Assay of Antibodies to Adult T-cell Leukemia-Associated Antigen. *Jpn. J. Cancer Res.* **1983**, *74*, 185–187.
8. Gallo, D.; Hoffman, M. N.; Cossen, C. K.; Diggs, J. L.; Hurst, J. W.; Penning, L. M. Comparison of Immunofluorescence, Enzyme Immunoassay, and Western Blot (Immunoblot) Methods for Detection of Antibody to Human T-cell Leukemia Virus Type I. *J. Clin. Microbiol.* **1988**, *26*, 1487–1491.
9. World Health Organization. Acquired Immunodeficiency Syndrome (AIDS): Proposed WHO Criteria for Interpreting Results from Western Blot Assays for HIV-1, HIV-2, and HTLV-I/HTLV-II. *Week Epidemiol. Rec.* **1990**.

10. Kamihira, S.; Dateki, N.; Sugahara, K.; Hayashi, T.; Harasawa, H.; Minami, S.; Hirakata, Y.; Yamada, Y. Significance of HTLV-1 Proviral Load Quantification by Real-Time PCR as a Surrogate Marker for HTLV-1-infected Cell Count. *Clin. Lab. Haem.* **2003**, *25*, 111–117.
11. Seiki, M.; Hattori, S.; Hirayama, Y.; Yoshida, M. Human Adult T-cell Leukemia Virus: Complete Nucleotide Sequence of the Provirus Genomes Integrated in Leukemia Cell DNA. *Proc. Natl. Acad. Sci. USA* **1982**, *80*, 3618–3622.
12. Popovic, M.; Reitz, M. S.; Sangadharan, M. G.; Robert-Guroff, M.; Kalyanaraman, V. S.; Nakao, Y.; Miyoshi, I.; Minowada, J.; Yoshida, M.; Ito, Y.; Gallo, R. C. The Virus of Japanese Adult T-cell Leukaemia is a Member of the Human T-cell Leukaemia Virus Group. *Nature* **1982**, *300*, 63–66.
13. Iwanaga, M.; Watanabe, T.; Utsunomiya, A.; Okayama, A.; Uchimaru, K.; Koh, K. R.; Ogata, M.; Kikuchi, H.; Sagara, Y.; Uozumi, K.; Mochizuki, M.; Tsukasaki, K.; Saburi, Y.; Yamamura, M.; Tanaka, J.; Moriuchi, Y.; Hino, S.; Kamihira, S.; Yamaguchi, K. Human T-cell Leukemia Virus Type I (HTLV-1) Proviral Load and Disease Progression in Asymptomatic HTLV-1 Carriers: A Nationwide Prospective Study in Japan. *Blood* **2010**, *116*, 1211–1219.
14. Kamihira, S.; Yamano, Y.; Iwanaga, M.; Sasaki, D.; Satake, M.; Okayama, A.; Umeki, K.; Kubota, R.; Izumo, S.; Yamaguchi, K.; Watanabe, T. Intra- and Inter-Laboratory Variability in Human T-cell Leukemia Virus Type-1 Proviral Load Quantification using Real-Time Polymerase Chain Reaction Assays: A Multi-Center Study. *Cancer Sci.* **2010**, *101*(11), 2361–2367.
15. Osame, M.; Usuku, K.; Izumo, S.; Ijichi, N.; Amitania, H.; Igata, A.; Matsumoto, M.; Tara, M. HTLV-I-associated Myelopathy: A New Clinical Entity. *Lancet* **1986**, *i*, 1031–1032.
16. Usuku, K.; Sonoda, S.; Osame, M.; Yashiki, S.; Takahashi, K.; Matsumoto, M.; Sawada, T.; Tsuji, K.; Tara, M.; Igata, A. HLA Haplotype-linked High Immune Responsiveness against HTLV-I in HTLV-I-associated Myelopathy: Comparison with Adult T-cell Leukemia/Lymphoma. *Ann. Neurol.* **1988**, *23*(suppl), S143–150.
17. Koga, Y.; Iwanaga, M.; Soda, M.; Inokuchi, N.; Sasaki, D.; Hasegawa, H.; Yanagihara, K.; Yamaguchi, K.; Kamihira, S.; Yamada, Y. Trends in HTLV-1 Prevalence and Incidence of Adult T-cell Leukemia/Lymphoma in Nagasaki, Japan. *J. Med. Virol.* **2010**, *82*(4), 668–674.
18. Hino, S.; Katamine, S.; Miyata, H. et al. Primary Prevention of HTLV-1 in Japan. *Leukemia* **1997**, *11*, S57–59.
19. Takahashi, T.; Takezaki, T.; Oki, T.; Kawakamin, K.; Yashiki, S.; Fujiyoshi, T.; Usuku, K.; Mueller, N.; Osame, M.; Miyata, K. Inhibitory Effect of Maternal Antibody on Mother-to-Child Transmission of Human T-lymphotropic Virus Type I. *Int. J. Cancer* **1991**, *49*, 673–677.
20. Ando, Y.; Nakano, S.; Saito, K.; Shimamoto, I.; Ichijo, M.; Toyama, T.; Hinuma, Y. Prevention of HTLV-I Transmission through the Breast Milk by a Freeze-Thawing Process. *Jpn. J. Cancer Res.* **1986**, *77*, 974–977.
21. Kusuhara, K.; Sonoda, S.; Takahashi, K.; Tokugawa, K.; Fukushige, J.; Ueda, K. Mother-to-Child Transmission of Human T-cell Leukemia Virus Type I (HTLV-I): A Fifteen-Year Follow-up Study in Okinawa. *Jpn. Int. J. Cancer* **1987**, *40*, 755–757.
22. Tsuji, Y.; Doi, H.; Yamabe, T.; Ishimaru, T.; Miyamoto, T.; Hino, S. Prevention of Mother-to-Child Transmission of Human T-lymphotropic Virus Type-I. *Pediatrics* **1990**, *86*(1), 11–17.
23. Naderi, M.; Paryan, M.; Azadmanesh, K.; Rafatpanah, H.; Rezvan, H.; Mirab Samiee, S. Design and Development of a Quantitative Real Time PCR Assay for Monitoring of HTLV-1 Provirus in Whole Blood. *J. Clin. Virol.* **2012**, *53*(4), 302–307.
24. Lee, T. H.; Chafets, D. M.; Busch, M. P.; Murphy, E. L. Quantitation of HTLV-I and II Proviral Load using Real-Time Quantitative PCR with SYBR Green Chemistry. *J. Clin. Virol.* **2004**, *31*(4), 275–282.
25. Césaire, R.; Dehée, A.; Lézin, A.; Désiré, N.; Bourdonné, O.; Dantin, F.; Béra, O.; Smadja, D.; Abel, S.; Cabié, A.; Sobesky, G.; Nicolas, J. C. Quantification of HTLV Type I and HIV Type I DNA Load in Coinfected Patients: HIV Type 1 Infection Does not Alter HTLV Type I Proviral Amount in the Peripheral Blood Compartment. *AIDS Res. Hum. Retrovir.* **2001**, *17*(9), 799–805.
26. Kamihira, S.; Dateki, N.; Sugahara, K.; Yamada, Y.; Tomonaga, M.; Maeda, T.; Tahara, M. Real-Time Polymerase Chain Reaction for Quantification of HTLV-1 Proviral Load: Application for Analyzing Aberrant Integration of the Proviral DNA in Adult T-cell Leukemia. *Int. J. Hematol.* **2000**, *72*(1), 79–84.
27. Dehée, A.; Césaire, R.; Désiré, N.; Lézin, A.; Bourdonné, O.; Béra, O.; Plumelle, Y.; Smadja, D.; Nicolas, J. C. Quantitation of HTLV-I Proviral Load by a TaqMan Real-Time PCR Assay. *J. Virol. Meth.* **2002**, *102*(1–2), 37–51.

The NEW ENGLAND JOURNAL of MEDICINE

ORIGINAL ARTICLE

Genetic Variants in C5 and Poor Response to Eculizumab

Jun-ichi Nishimura, M.D., Ph.D., Masaki Yamamoto, M.D., Shin Hayashi, M.D., Ph.D., Kazuma Ohyashiki, M.D., Ph.D., Kiyoshi Ando, M.D., Ph.D., Andres L. Brodsky, M.D., Ph.D., Hideyoshi Noji, M.D., Kunio Kitamura, M.D., Ph.D., Tetsuya Eto, M.D., Toru Takahashi, M.D., Masayoshi Masuko, M.D., Ph.D., Takuro Matsumoto, M.D., Yuji Wano, M.D., Tsutomu Shichishima, M.D., Ph.D., Hirohiko Shibayama, M.D., Ph.D., Masakazu Hase, Ph.D., Lan Li, M.D., Krista Johnson, M.Sc., Alberto Lazarowski, Ph.D., Paul Tamburini, Ph.D., Johji Inazawa, M.D., Ph.D., Taroh Kinoshita, Ph.D., and Yuzuru Kanakura, M.D., Ph.D.

ABSTRACT

BACKGROUND

Eculizumab is a humanized monoclonal antibody that targets complement protein C5 and inhibits terminal complement–mediated hemolysis associated with paroxysmal nocturnal hemoglobinuria (PNH). The molecular basis for the poor response to eculizumab in a small population of Japanese patients is unclear.

METHODS

We assessed the sequences of the gene encoding C5 in patients with PNH who had either a good or poor response to eculizumab. We also evaluated the functional properties of C5 as it was encoded in these patients.

RESULTS

Of 345 Japanese patients with PNH who received eculizumab, 11 patients had a poor response. All 11 had a single missense C5 heterozygous mutation, c.2654G→A, which predicts the polymorphism p.Arg885His. The prevalence of this mutation among the patients with PNH (3.2%) was similar to that among healthy Japanese persons (3.5%). This polymorphism was also identified in a Han Chinese population. A patient in Argentina of Asian ancestry who had a poor response had a very similar mutation, c.2653C→T, which predicts p.Arg885Cys. Nonmutant and mutant C5 both caused hemolysis in vitro, but only nonmutant C5 bound to and was blocked by eculizumab. In vitro hemolysis due to nonmutant and mutant C5 was completely blocked with the use of N19-8, a monoclonal antibody that binds to a different site on C5 than does eculizumab.

CONCLUSIONS

The functional capacity of C5 variants with mutations at Arg885, together with their failure to undergo blockade by eculizumab, account for the poor response to this agent in patients who carry these mutations. (Funded by Alexion Pharmaceuticals and the Ministry of Health, Labor, and Welfare of Japan.)

From Osaka University Graduate School of Medicine (J.N., M.Y., H.S., Y.K.) and World Premier International Immunology Frontier Research Center and Research Institute for Microbial Diseases, Osaka University, Suita (T.K.), Medical Research Institute and Hard Tissue Genome Research Center, Tokyo Medical and Dental University (S.H., J.I.), Tokyo Medical University (K.O.), and Alexion Pharma (M.H.), Tokyo, Tokai University School of Medicine, Isehara (K.A.), Fukushima Medical University, Fukushima (H.N., T.S.), Ichinomiya Municipal Hospital, Ichinomiya (K.K.), Hamanomachi Hospital, Fukuoka (T.E.), Yamaguchi Grand Medical Center, Hofu (T.T.), Niigata University Medical and Dental Hospital, Niigata (M.M.), Japanese Red Cross Takayama Hospital, Takayama (T.M.), and Iwate Prefectual Central Hospital, Morioka (Y.W.) — all in Japan; University of Buenos Aires, Buenos Aires (A.L.B., A.L.); and Alexion Pharmaceuticals, Cheshire, CT (L.L., K.J., P.T.). Address reprint requests to Dr. Nishimura at the Department of Hematology and Oncology, Osaka University Graduate School of Medicine, 2-2 Yamadaoka, Suita, Osaka 565-0871, Japan, or at junnishi@bldon.med.osaka-u.ac.jp.

Drs. Nishimura and Yamamoto contributed equally to this article.

N Engl J Med 2014;370:632-9.
DOI: 10.1056/NEJMoa1311084

PAROXYSMAL NOCTURNAL HEMOGLOBINuria (PNH) arises as a consequence of clonal expansion of hematopoietic stem cells that have acquired a somatic mutation in the gene encoding phosphatidylinositol glycan anchor biosynthesis class A (*PIGA*).[1-3] The resulting hematopoietic cells are deficient in glycosylphosphatidylinositol-anchored proteins, including the complement regulatory proteins CD55 and CD59; this accounts for the intravascular hemolysis that is the primary clinical manifestation of PNH.[4-6] PNH frequently develops in association with disorders involving bone marrow failure, particularly aplastic anemia. Thrombosis is a major cause of PNH-associated morbidity and mortality, particularly among white patients.[7-9]

Eculizumab (Soliris, Alexion Pharmaceuticals) is a humanized monoclonal antibody that specifically binds to the terminal complement protein C5, inhibiting its cleavage into C5a and C5b by C5 convertases and thereby preventing the release of the inflammatory mediator C5a and the formation of the cytolytic pore C5b–9.[10,11] C5 blockade preserves the critical immune-protective and immune-regulatory functions of upstream components that culminate in C3b-mediated opsonization and immune clearance. Eculizumab is highly effective in reducing intravascular hemolysis in PNH; it decreases or eliminates the need for blood transfusion, improves quality of life, and reduces the risk of thrombosis among both patients with classic PNH and those in whom PNH develops secondary to aplastic anemia.[12-16]

Since the approval of eculizumab by regulatory authorities outside Japan, more than 99% of patients in whom it has been administered have had a good response with respect to decreases in intravascular hemolysis.[12-16] However, in the Japanese AEGIS study of eculizumab in patients with PNH, 2 of 29 patients had a poor response.[17] In those 2 patients, the level of lactate dehydrogenase (LDH) remained markedly high during treatment with eculizumab. As of this writing, 345 Japanese patients have received eculizumab, and 11 patients who share the same single polymorphism and who have had a poor response (3.2%) have been identified. In this study (C07-001: Safety and Efficacy Study of Eculizumab in Paroxysmal Nocturnal Hemoglobinuria Patients), we sought to elucidate the molecular basis for the poor response in this small subgroup of Japanese patients with PNH.

METHODS

STUDY OVERSIGHT

The study was sponsored by Alexion Pharmaceuticals and the Ministry of Health, Labor, and Welfare of Japan. The first and last authors had final responsibility for the study design, oversight, and data verification and analyses. Written informed consent was obtained from all patients according to the Declaration of Helsinki. Approval for the study was obtained from the institutional review board at each study site. All the authors collected and maintained the data. Members of the academic steering committee in conjunction with the sponsor contributed to the interpretation of the results, wrote the first version of the manuscript and approved all versions, made the decision to submit the manuscript for publication, and vouch for the accuracy and completeness of the data reported and the fidelity of this article to the study protocol, which is available with the full text of this article at NEJM.org. Alexion Pharmaceuticals and Infusion Communications provided medical-writing support.

PATIENTS

Blood samples were obtained from 12 patients (11 Japanese patients and 1 Argentinian patient of Asian ancestry) identified as having a poor response to eculizumab. A poor response was defined as markedly high levels of LDH during treatment, indicating that intravascular hemolysis remained unaffected, regardless of whether there were improvements in other laboratory findings or clinical symptoms. This condition is distinct from mechanisms of extravascular hemolysis that occur in some patients during treatment with eculizumab, as reported by another group.[18] Control samples from 1 healthy person and 7 patients with PNH who had a good response to eculizumab were also obtained. All blood samples were collected by means of venipuncture.

HEMOLYTIC ASSAYS

We determined the pharmacodynamic response to eculizumab by measuring the capacity of the patients' serum to lyse antibody-sensitized chicken erythrocytes in a human serum-complement hemolytic assay.[12] Less than 20% residual hemoly-

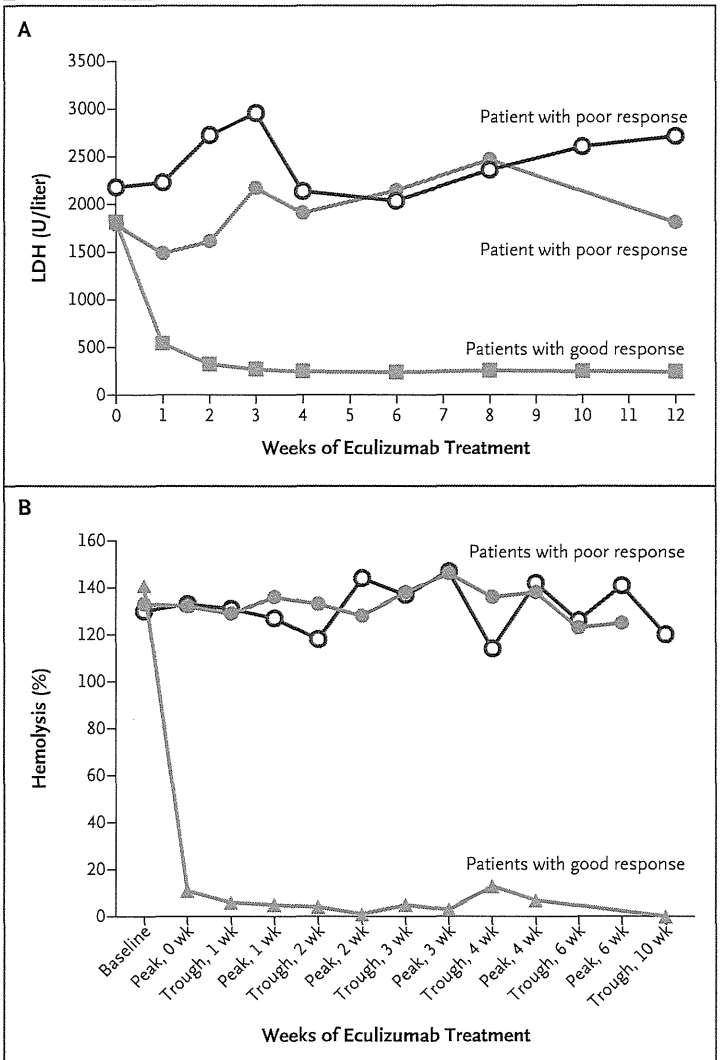

Figure 1. Pharmacodynamic Analysis of Eculizumab in 2 Patients with a Poor Response and in 27 Patients with a Good Response in the AEGIS Study.

Panel A shows levels of lactate dehydrogenase (LDH), which remained elevated during the 12-week treatment period in the 2 patients with a poor response to eculizumab, whereas they returned to almost normal values in 27 patients with a good response. Panel B shows in vitro hemolytic activity in serum samples obtained from the patients. In the 2 patients with a poor response, the level of hemolysis, like the LDH level, was unaffected by treatment with eculizumab, whereas in patients with a good response, hemolytic activity was completely suppressed throughout the treatment period.

sis is indicative of complete blockade of hemolysis in this assay system. N19-8, an anti-C5 monoclonal antibody that binds to a different site on C5 than eculizumab,[19] was used instead of eculizumab in some hemolytic assays.

C5 GENE SEQUENCING

Genomic DNA was isolated from peripheral-blood mononuclear cells with the use of the DNeasy Blood and Tissue Kit (Qiagen), and messenger RNA (mRNA) was isolated from peripheral-blood mononuclear cells with the use of the QIAamp RNA Blood Mini Kit (Qiagen). We synthesized complementary DNA (cDNA) from the mRNA using high-capacity cDNA reverse-transcription kits (Applied Biosystems).

The C5 gene consists of 41 exons that contain a total of 97,942 bp. To cover each exon, we designed 41 specific primer sets at introns flanking each of the 41 exons according to the C5 gene sequences reported in the GenBank database (GenBank accession number, NG_007364.1). Primer sequences for exon 21, which contains the identified mutations, are shown in Figure S1 in the Supplementary Appendix (available at NEJM.org). Total genomic DNA was used as a template and was amplified with the use of a polymerase-chain-reaction (PCR) assay. We sequenced the amplified fragments with the same primer pair, using the BigDye Terminator, version 1.1, cycle sequencing kit (Applied Biosystems).

SCREENING FOR MUTATIONS IN C5

To determine the prevalence of a heterozygous point mutation, c.2654G→A, in the healthy Japanese population, the PCR product (185 bp) derived from peripheral blood for the nucleotide sequences at exon 21 was digested with the use of the *Apa*LI restriction enzyme, and digested samples were separated by means of electrophoresis in 2% agarose gel. To analyze the distribution of the identified variants, c.2654G→A and c.2653C→T, in various populations, we sequenced the PCR product using the Sanger method. DNA panels containing samples obtained from 100 persons from England and Scotland (panel MGP00003), 120 Han Chinese persons (panel MGP00017), and 90 persons in Los Angeles who were of Mexican ancestry (HapMap [release 13]) were purchased (Coriell Institute for Medical Research).

GENERATION OF RECOMBINANT C5

Recombinant nonmutant human C5 (rC5) was derived from the nonmutant gene cloned into an expression vector, pEE12.4. Recombinant mutant C5 (rC5m) was created from rC5 by

means of site-directed mutagenesis (Stratagene QuikChange Lightning kit, Agilent Technologies). Both rC5 and rC5m were expressed in 293 cells with the use of the transient Expi293 expression system (Invitrogen) and were purified from the tissue-culture expression medium according to a modification of a previously described method.[20] Recombinant C5 was quantified with the use of a bicinchoninic assay (Pierce Biotechnology), evaluated by means of sodium dodecyl sulfate–polyacrylamide gel electrophoresis and a laboratory-on-a-chip capillary electrophoresis (Protein 230 kit, Agilent), and stored at −80°C. Final preparations of both rC5 and rC5m were more than 95% pure.

BINDING AFFINITY ASSAY

Surface-plasmon-resonance analysis (Biacore 3000) was used to assess the binding of eculizumab to C5 with the use of an antihuman IgG (Fc) capture method. Antihuman IgG (Fc) (KPL 01-10-20) diluted to 0.1 mg per milliliter in 10-mM sodium acetate (pH 5.0) was immobilized on two flow cells of a CM5 sensor chip for 8 minutes by means of amine coupling. Eculizumab was diluted to 0.25 μg per milliliter in running buffer (10 mM HEPES buffer, 150 mM sodium chloride, 3 mM EDTA, and 0.005% polysorbate 20, pH 7.4). One flow cell was used as a reference. Diluted antibody was then injected onto the other flow cell, followed by injection of rC5 or rC5m at concentrations ranging from 4 nM to 1 μM. The surface was regenerated each time with 20 mM hydrochloric acid and 0.01% polysorbate 20 (100 μl per minute, 200-μl injection).

RESULTS

PATIENTS WITH A POOR RESPONSE IN THE AEGIS STUDY

During the 12-week period of eculizumab treatment in the AEGIS study, two patients with PNH had markedly elevated levels of LDH that did not decrease, suggesting that eculizumab did not protect the erythrocytes in these two patients from uncontrolled complement activation (Fig. 1A, and Table S1 in the Supplementary Appendix). This was confirmed in a subsequent analysis of pharmacokinetics and pharmacodynamics. Thus, despite the fact that peak and trough levels of eculizumab during the study remained well above the minimal level required to completely inhibit complement-mediated hemolysis in patients with PNH (>35 μg per milliliter) (Fig. S2 in the Supplementary Appendix), rates of hemolysis in the two patients with a poor response were unaffected under conditions in which hemolytic

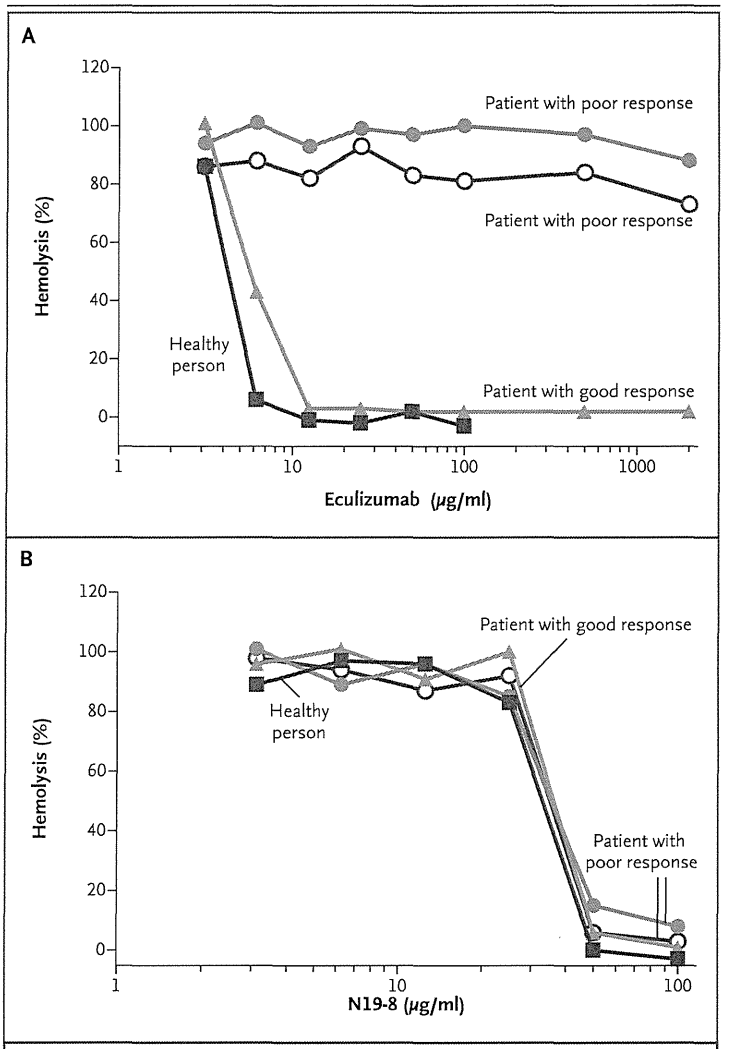

Figure 2. Effect of Exogenous Eculizumab and a Different Anti-C5 Antibody (N19-8) on Hemolytic Activity in Serum Samples Obtained from Patients before the Administration of Eculizumab.

Panel A shows the effect of the addition of exogenous eculizumab on in vitro hemolysis. Exogenous eculizumab, up to a final concentration of 2000 μg per milliliter, did not inhibit in vitro hemolysis in the serum samples obtained before administration of the drug in two patients with a poor response, whereas inhibition was seen in serum samples obtained from a patient with a good response and a healthy person. In contrast, as shown in Panel B, an anti-C5 antibody to a different epitope (N19-8) suppressed complement-mediated in vitro hemolysis in all the samples obtained from the same four persons.

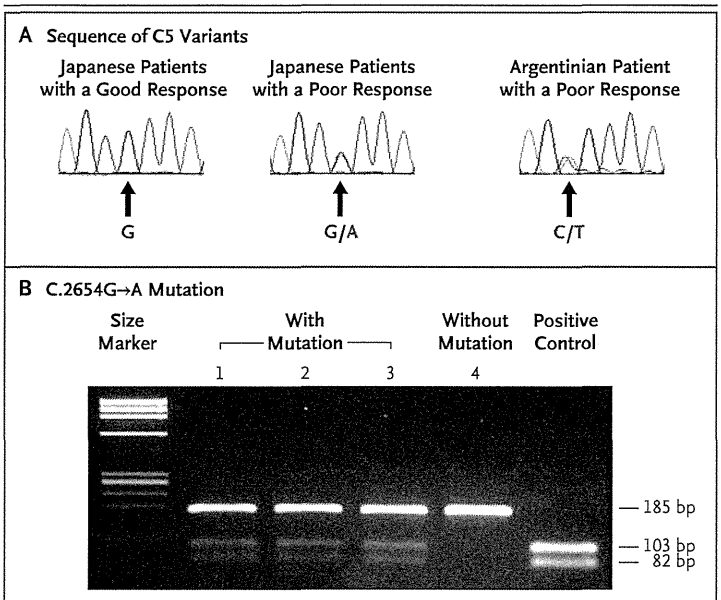

Figure 3. Genetic Variants of C5.

Panel A shows the sequence of the C5 variants detected in Japanese patients and an Argentinian patient with a poor response to eculizumab, as compared with the more frequently observed sequence in patients who had a good response to the drug. A heterozygous missense mutation in exon 21, c.2654G→A, predicting p.Arg885His, was identified in all Japanese patients with a poor response but not in those who had a good response. A very similar mutation, c.2653C→T, which predicts p.Arg885Cys, was identified in an Argentinian patient of Asian ancestry who had a poor response. Panel B shows a typical 2% agarose gel analysis to detect the presence of the c.2654G→A mutation. This mutation creates an *Apa*LI recognition site, which, when digested with *Apa*LI, generates the 185-bp polymerase-chain-reaction (PCR) product and two additional DNA fragments of 103 bp and 82 bp in length in heterozygous persons (lanes 1, 2, and 3). Lane 4 shows a PCR product from a homozygous sample without the mutation. The PCR product derived from a plasmid inserted with the mutant sequence was used as a positive control.

activity was completely suppressed in the patients with a good response (Fig. 1B).

These observations were corroborated through further study of the effect of exogenous eculizumab on the hemolytic activity in a serum sample obtained from a patient before administration of the drug. Although in vitro hemolytic activity in serum samples obtained from a healthy person and from a patient who had a good response to eculizumab was completely inhibited by eculizumab at serum concentrations of 6.25 μg per milliliter and 12.5 μg per milliliter, respectively, levels as high as 2000 μg of eculizumab per milliliter did not inhibit in vitro hemolysis in the serum samples obtained from the two patients who had a poor response (Fig. 2A). In contrast, results with N19-8, an antibody that binds a site on C5 that is distinct from the eculizumab binding site, showed that suppression of complement-mediated hemolysis was similar in the healthy person, the patient who had a good response to eculizumab, and the two patients who had a poor response (Fig. 2B).

C5 MUTATION IN JAPANESE PATIENTS WITH A POOR RESPONSE

We amplified all 41 exons of the C5 gene with primer sets specifically designed for each exon, using as a template genomic DNA prepared from mononuclear cells obtained from patients who had a poor response, and we directly sequenced all the PCR products from each exon (Fig. S1 in the Supplementary Appendix). We identified a single missense C5 heterozygous mutation at exon 21, c.2654G→A (DNA Data Bank of Japan accession number, AB860298), which predicts the polymorphism p.Arg885His, in both patients who had a poor response. This mutation was not seen in 7 patients who had a good response to eculizumab (Fig. 3A). In addition, we confirmed that 9 other Japanese patients who received treatment after completion of the AEGIS study and who had a poor response to eculizumab had the same C5 gene mutation (Table S1 in the Supplementary Appendix). The 11 patients with a poor response who had this mutation were identified among 345 Japanese patients who received eculizumab (rate of a poor response, 3.2%).

The c.2654G→A mutation generates a new *Apa*LI recognition site (Fig. S3 in the Supplementary Appendix); therefore, when digested with *Apa*LI, the 185-bp PCR product of exon 21 associated with nonmutant C5 generates two DNA fragments of 103 bp and 82 bp in length (Fig. 3B). However, the *Apa*LI digestion products from all 11 patients who had a poor response contained a mixture of the 185-, 103-, and 82-bp fragments; this confirms that each of these patients was heterozygous, with c.2654G→A in one allele and a nonmutant sequence in the other allele.

Next, we analyzed the prevalence of this mutation in the healthy Japanese population, using the gel-based assay in conjunction with DNA samples. We found that 10 of 288 healthy persons in Japan had the same heterozygous muta-

tion (3.5%), which is consistent with the prevalence we observed in the population of Japanese patients with PNH.

To determine the distribution of this polymorphism in other racial and ethnic populations, we screened several DNA panels. The c.2654G→A polymorphism was identified in 1 of 120 Han Chinese persons but was not seen in samples obtained from 100 persons of British ancestry and from 90 persons of Mexican ancestry.

MUTANT C5 IN JAPANESE PATIENTS WITH A POOR RESPONSE

To assess the influence of the genetic change on C5 function, electrophoretically pure rC5 and rC5m containing c.2654G→A were generated and functionally compared in various in vitro experiments. As a preliminary experiment, we confirmed that natural C5 (nC5), rC5, and rC5m restored classical-pathway lysis equivalently when added to C5-depleted serum (data not shown). Eculizumab did not block classical-pathway lysis in serum reconstituted with rC5m but did block rC5-dependent and nC5-dependent lysis (Fig. S4A in the Supplementary Appendix). By contrast, as observed with serum samples obtained from patients, N19-8 inhibited lysis in C5-depleted serum reconstituted with nC5, rC5, and rC5m (Fig. S4B in the Supplementary Appendix). Finally, although eculizumab bound nanomolar concentrations of rC5 on surface-plasmon-resonance analysis, with clear association and dissociation phases, there was no detectable binding with rC5m in the same assay up to the highest concentration of eculizumab (1 μM) examined (Fig. 4).

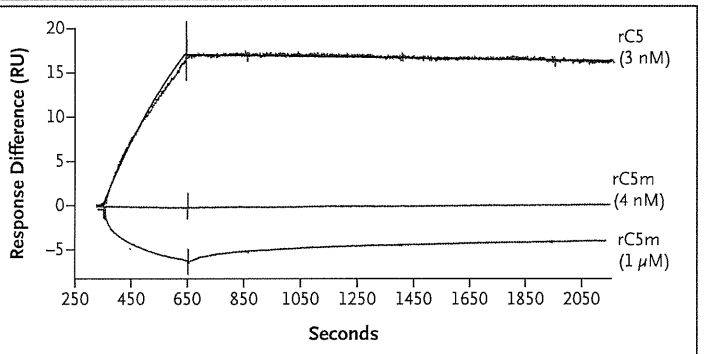

Figure 4. Effect of the Japanese C5 Polymorphism on the Functional Properties of C5.

Binding of eculizumab to recombinant C5 (rC5) with and without the mutation, as assessed by means of surface plasmon resonance, is shown. Eculizumab bound rC5 but did not bind mutant rC5 (rC5m) at concentrations below 5 nM. Increasing the concentration of eculizumab up to 1 μM did not elicit detectable binding to rC5m. A response unit (RU) is 1 pg of protein per square millimeter on a sensor surface. The vertical line at 650 seconds separates the on and off phases of the kinetics experiment (association of the analyte with dissociation from the ligand).

C5 MUTATION IN AN ARGENTINIAN PATIENT WITH A POOR RESPONSE

One patient with a poor response to eculizumab in whom the level of LDH remained markedly high during treatment with eculizumab was referred to us from Argentina. Although the known C5 polymorphism, c.2654G→A, was not identified in this patient, a new mutation, c.2653C→T, which predicts p.Arg885Cys, was detected in the base next to the known polymorphism (Fig. 3A).

To determine the prevalence and the distribution of this new variant, the same DNA panels described above were screened, but no mutation was identified in the 120 Han Chinese persons, the 100 persons of British ancestry, or the 90 persons of Mexican ancestry, suggesting that the prevalence of this variant might be too low to be detected in a sample of this size.

DISCUSSION

We identified a C5 mutation in Japanese patients with PNH. This mutation prevents binding and blockade by eculizumab while retaining the functional capacity of the mutant C5 to cause hemolysis.

Two patients with PNH enrolled in the AEGIS clinical trial did not have the characteristic response to eculizumab treatment, as shown by the lack of change in hemolytic markers such as levels of LDH. Serum samples obtained from these patients showed hemolytic activity even in the presence of high concentrations of exogenously added eculizumab. However, hemolytic activity was completely blocked by another anti-C5 monoclonal antibody (N19-8), which binds to a different site from that of eculizumab. A single missense C5 heterozygous mutation, c.2654G→A, was consistently detected in all 11 Japanese patients with a poor response and in none of the patients who had a good response. The prevalence of this polymorphism among patients with PNH (3.2%) was very similar to the prevalence

in healthy Japanese persons (3.5%), and the polymorphism has been identified in 1 of 120 Han Chinese persons. We then showed that the hemolytic activity supported by this structural variant in vitro was not blocked by eculizumab but was fully blocked by N19-8 and that the variant was incapable of binding eculizumab. Collectively, these data provide support for the hypothesis that the functional capacity of the mutant C5, together with its inability to bind to eculizumab, account for the poor response in patients who carry this mutation.

A new variant, c.2653C→T, which predicts p.Arg885Cys, was independently identified in an Argentinian patient of Asian ancestry, suggesting the importance of this site in C5 recognition by eculizumab and the racial and ethnic factors associated with this phenomenon. The Arg885His/Cys mutations are proximal to the C5 MG7 domain, close to the known epitope for binding of eculizumab[21] and within the contact region between the C5 convertase and bound C5 substrate, as inferred by Laursen et al.[22] Evidently, these mutations, in keeping with the high specificity of monoclonal antibody binding, disrupt the eculizumab epitope but maintain the capacity of C5m to undergo cleavage by the C5 convertase. Therefore, we conclude that the poor response to eculizumab in a subgroup of Japanese patients is explained by the inability of a subset of lysis-competent C5 in these patients to bind and undergo blockade by the drug. The polymorphism in the target protein might be important to consider in patients with a poor response to other antibody-based treatments for various diseases.[23-25]

Supported by Alexion Pharmaceuticals and a grant from the Research Committee for the Idiopathic Hematopoietic Disorders, Ministry of Health, Labor, and Welfare of Japan (H23-Nanchi-Japan-001).

Disclosure forms provided by the authors are available with the full text of this article at NEJM.org.

We thank the following employees of Alexion Pharmaceuticals for technical support: Richard Altman and Doug Sheridan (for assistance with protein expression), Fang Sun (for assistance with protein purification), Rekha Patel (for assistance with surface-plasmon-resonance analysis), and Gerard Graminski (for assistance with bioanalytical assays); Drs. Yoshiko Murakami and Yusuke Maeda, both of Osaka University, Japan, for advice and critical discussions; and Dr. Otto Götze of the Department of Immunology, University of Göttingen, Germany, for supplying the hybridoma cells for N19-8.

REFERENCES

1. Miyata T, Takeda J, Iida Y, et al. The cloning of PIG-A, a component in the early step of GPI-anchor biosynthesis. Science 1993;259:1318-20.
2. Takeda J, Miyata T, Kawagoe K, et al. Deficiency of the GPI anchor caused by a somatic mutation of the PIG-A gene in paroxysmal nocturnal hemoglobinuria. Cell 1993;73:703-11.
3. Miyata T, Yamada N, Iida Y, et al. Abnormalities of PIG-A transcripts in granulocytes from patients with paroxysmal nocturnal hemoglobinuria. N Engl J Med 1994;330:249-55.
4. Parker C, Omine M, Richards S, et al. Diagnosis and management of paroxysmal nocturnal hemoglobinuria. Blood 2005;106:3699-709.
5. Brodsky RA. How I treat paroxysmal nocturnal hemoglobinuria. Blood 2009; 113:6522-7.
6. Luzzatto L, Gianfaldoni G, Notaro R. Management of paroxysmal nocturnal haemoglobinuria: a personal view. Br J Haematol 2011;153:709-20.
7. Hillmen P, Lewis SM, Bessler M, Luzzatto L, Dacie JV. Natural history of paroxysmal nocturnal hemoglobinuria. N Engl J Med 1995;333:1253-8.
8. Socié G, Mary JY, de Gramont A, et al. Paroxysmal nocturnal haemoglobinuria: long-term follow-up and prognostic factors. Lancet 1996;348:573-7.
9. Nishimura J, Kanakura Y, Ware RE, et al. Clinical course and flow cytometric analysis of paroxysmal nocturnal hemoglobinuria in the United States and Japan. Medicine (Baltimore) 2004;83:193-207.
10. Rother RP, Rollins SA, Mojcik CF, Brodsky RA, Bell L. Discovery and development of the complement inhibitor eculizumab for the treatment of paroxysmal nocturnal hemoglobinuria. Nat Biotechnol 2007;25:1256-64. [Erratum, Nat Biotechnol 2007;25:1488.]
11. Parker C. Eculizumab for paroxysmal nocturnal haemoglobinuria. Lancet 2009; 373:759-67.
12. Hillmen P, Hall C, Marsh JC, et al. Effect of eculizumab on hemolysis and transfusion requirements in patients with paroxysmal nocturnal hemoglobinuria. N Engl J Med 2004;350:552-9.
13. Hill A, Hillmen P, Richards SJ, et al. Sustained response and long-term safety of eculizumab in paroxysmal nocturnal hemoglobinuria. Blood 2005;106:2559-65.
14. Hillmen P, Young NS, Schubert J, et al. The complement inhibitor eculizumab in paroxysmal nocturnal hemoglobinuria. N Engl J Med 2006;355:1233-43.
15. Hillmen P, Muus P, Dührsen U, et al. Effect of the complement inhibitor eculizumab on thromboembolism in patients with paroxysmal nocturnal hemoglobinuria. Blood 2007;110:4123-8.
16. Brodsky RA, Young NS, Antonioli E, et al. Multicenter phase 3 study of the complement inhibitor eculizumab for the treatment of patients with paroxysmal nocturnal hemoglobinuria. Blood 2008; 111:1840-7.
17. Kanakura Y, Ohyashiki K, Shichishima T, et al. Safety and efficacy of the terminal complement inhibitor eculizumab in Japanese patients with paroxysmal nocturnal hemoglobinuria: the AEGIS clinical trial. Int J Hematol 2011;93:36-46.
18. Risitano AM, Notaro R, Marando L, et al. Complement fraction 3 binding on erythrocytes as additional mechanism of disease in paroxysmal nocturnal hemoglobinuria patients treated by eculizumab. Blood 2009;113:4094-100.
19. Würzner R, Schulze M, Happe L, et al. Inhibition of terminal complement complex formation and cell lysis by monoclonal antibodies. Complement Inflamm 1991;8:328-40.
20. van den Berg CW. Purification of complement components, regulators, and receptors by classical methods. Methods Mol Biol 2000;150:15-52.
21. Zuber J, Fakhouri F, Roumenina LT, Loirat C, Frémeaux-Bacchi V. Use of eculizumab for atypical haemolytic uraemic syndrome and C3 glomerulopathies. Nat Rev Nephrol 2012;8:643-57.
22. Laursen NS, Andersen KR, Braren I,

Spillner E, Sottrup-Jensen L, Andersen GR. Substrate recognition by complement convertases revealed in the C5-cobra venom factor complex. EMBO J 2011;30:606-16.
23. Wu J, Edberg JC, Redecha PB, et al. A novel polymorphism of FcgammaRIIIa (CD16) alters receptor function and predisposes to autoimmune disease. J Clin Invest 1997;100:1059-70.
24. Cartron G, Dacheux L, Salles G, et al. Therapeutic activity of humanized anti-CD20 monoclonal antibody and polymorphism in IgG Fc receptor FcgammaRIIIa gene. Blood 2002;99:754-8.
25. Treon SP, Hansen M, Branagan AR, et al. Polymorphisms in FcgammaRIIIA (CD16) receptor expression are associated with clinical response to rituximab in Waldenström's macroglobulinemia. J Clin Oncol 2005;23:474-81.

Journal of General Virology (2014), 95, 179–189 DOI 10.1099/vir.0.057364-0

Poly-proline motif in HIV-2 Vpx is critical for its efficient translation

Ariko Miyake,[1]† Mikako Fujita,[2]† Haruna Fujino,[3] Ryoko Koga,[3] Sogo Kawamura,[3] Masami Otsuka,[3] Hirotaka Ode,[4,5] Yasumasa Iwatani,[4] Yosuke Sakai,[1] Naoya Doi,[1,5] Masako Nomaguchi,[1] Akio Adachi[1] and Yasuyuki Miyazaki[1]

Correspondence
Akio Adachi
adachi@basic.med.tokushima-u.ac.jp
Yasuyuki Miyazaki
ymiyazaki@basic.med.tokushima-u.ac.jp

[1]Department of Microbiology, Institute of Health Biosciences, University of Tokushima Graduate School, Tokushima, Tokushima, Japan

[2]Research Institute for Drug Discovery, School of Pharmacy, Kumamoto University, Kumamoto, Kumamoto, Japan

[3]Department of Bioorganic Medicinal Chemistry, Faculty of Life Sciences, Kumamoto University, Kumamoto, Kumamoto, Japan

[4]Clinical Research Center, National Hospital Organization, Nagoya Medical Center, Nagoya, Aichi, Japan

[5]Japanese Foundation for AIDS Prevention, Chiyoda-ku, Tokyo, Japan

Human immunodeficiency virus type 2 (HIV-2) carries an accessory protein Vpx that is important for viral replication in natural target cells. In its C-terminal region, there is a highly conserved poly-proline motif (PPM) consisting of seven consecutive prolines, encoded in a poly-pyrimidine tract. We have previously shown that PPM is critical for Vpx expression and viral infectivity. To elucidate the molecular basis underlying this observation, we analysed the expression of Vpx proteins with various PPM mutations by *in vivo* and *in vitro* systems. We found that the number and position of consecutive prolines in PPM are important for Vpx expression, and demonstrated that PPM is essential for efficient Vpx translation. Furthermore, mutational analysis to synonymously disrupt the poly-pyrimidine tract suggested that the context of PPM amino acid sequences is required for efficient translation of Vpx. We similarly analysed HIV-1 and HIV-2 Vpr proteins structurally related to HIV-2 Vpx. Expression level of the two Vpr proteins lacking PPM was shown to be much lower relative to that of Vpx, and not meaningfully enhanced by introduction of PPM at the C terminus. Finally, we examined the Vpx of simian immunodeficiency virus from rhesus monkeys (SIVmac), which also has seven consecutive prolines, for PPM-dependent expression. A multi-substitution mutation in the PPM markedly reduced the expression level of SIVmac Vpx. Taken together, it can be concluded that the notable PPM sequence enhances the expression of Vpx proteins from viruses of the HIV-2/SIVmac group at the translational level.

Received 16 July 2013
Accepted 9 October 2013

INTRODUCTION

Primate immunodeficiency viruses carry a set of accessory proteins necessary for their optimal growth in host individuals (Blanco-Melo *et al.*, 2012; Harris *et al.*, 2012; Malim & Bieniasz, 2012; Zheng *et al.*, 2012). Extensive virological and molecular biological studies carried out so far have revealed that these auxiliary proteins profit the viruses mostly by antagonizing cellular antiviral restriction factors (Blanco-Melo *et al.*, 2012; Harris *et al.*, 2012; Malim & Bieniasz, 2012; Zheng *et al.*, 2012). One such viral protein, Vpx, is highly conserved among viruses of the human immunodeficiency virus type 2 (HIV-2) group, and plays a critical role in viral replication in different cell types (Fujita *et al.*, 2010). Vpx produced in cells is subsequently incorporated into progeny virions through a specific interaction of the putative third α-helix region (Jin *et al.*, 2001; Park & Sodroski, 1995) with the p6 domain of Gag (Accola *et al.*, 1999; Pancio & Ratner, 1998). The packaged Vpx then confers optimal infectivity on the virions in specific target cells such as macrophages and primary T-cells. Recently, it has been demonstrated that Vpx induces proteasomal degradation of host factors SAMHD1 (Hrecka *et al.*, 2011; Laguette *et al.*, 2011) and APOBEC3A (Berger *et al.*, 2011), relieving the restriction of virus infection.

†These authors contributed equally to this work.

Vpx presumably has three major α-helices and unstructured amino/carboxy termini like its paralogue Vpr (Khamsri *et al.*, 2006; Mahnke *et al.*, 2006), another accessory protein known to be abundantly virion-associated. Despite this similarity, there is a notable poly-proline motif (PPM) near the C terminus of Vpx (seven consecutive prolines in the Vpx proteins of HIV-2; simian immunodeficiency virus from rhesus monkeys, SIVmac; and SIV from sooty mangabey monkeys, SIVsmm), which is not present in Vpr. We have previously generated a series of proviral HIV-2 mutant clones and performed systemic virological studies on Vpx using primary macrophage cultures and a T-lymphocyte cell line as infection targets (Fujita *et al.*, 2008a, b, 2010; Ueno *et al.*, 2003). Although all 19 point mutants, with mutations scattered throughout the *vpx* gene, produced virions containing Vpx at a comparable level to a WT clone upon transfection, many of them were found to be defective for virus growth in macrophages and/or T-cells. The defective replication step of these mutants was shown to be in the early phase (before/during viral DNA synthesis and/or its nuclear import) by extensive virological and molecular analyses (Fujita *et al.*, 2008a, b, 2010; Ueno *et al.*, 2003). In contrast to above, the other two multi-substitution mutants of the proline stretch designated 103/4A and 106/4A (Fig. 1a) failed to express Vpx upon transfection and produced progeny virions without detectable Vpx (Fujita *et al.*, 2008a, b). Consistently, the two mutant viruses were growth-defective both in macrophages and T-cells (Fujita *et al.*, 2008b). In particular, the 106/4A mutant virus behaved exactly like a ΔVpx virus in infection experiments (Table 1). Although severely impeded, the 103/4A mutant virus was still infectious for macrophages and T-cells (Table 1). Because the expression of 103/4A and 106/4A Vpx proteins was below the detection level of the system used (Table 1), the reason for the different growth abilities of the two viruses remained to be determined. Notably, it has been shown that a PPM-deletion mutant, if expressed to some extent, retains Vpx functionality in single-round infection experiments (Goujon *et al.*, 2008; Gramberg *et al.*, 2010).

In this study, we have focused on the role of the PPM in Vpx expression and analysed the underlying molecular basis. Expression plasmids of HIV-2 Vpx with the PPM mutations were constructed for quantitative comparison and utilized for protein expression analysis using various cellular and *in vitro* cell-free translation systems. Our results demonstrated that the PPM in HIV-2 Vpx is critical for its efficient expression in the eukaryotic as well as prokaryotic translation machineries. In addition, we found that this effect is determined by the context of PPM amino acid sequences, but not the nucleotide sequences. These data support the notion that the PPM plays an important role in enhancing the translational level of HIV-2 Vpx in infected cells, thereby conferring optimal replication ability on the virus in target cells.

RESULTS

PPM in Vpx is critical for its efficient expression in cells

We have previously shown that the expression of Vpx in PPM mutants carrying P103/4A or P106/4A is at an undetectable level both in cells and in progeny virions produced from transiently transfected cells (Table 1). However, while the 106/4A mutant virus exhibited a ΔVpx growth-like phenotype in lymphocytic HSC-F cells and no viral growth in macrophages, the 103/4A mutant virus grew better in both cell types than the ΔVpx virus (Table 1). These results led us to assume that the expression plasmid, pME18Neo-Fvpx, used in the study (Fujita *et al.*, 2008b) was unable to efficiently express the protein. Therefore, we have constructed a new expression plasmid based on pEF1/*myc*-HisA (pEF-Fvpx in Fig. 1b), and compared its ability with the old version (pME18Neo-Fvpx in Fig. 1b). As clearly observed in Fig. 1(b), pEF-Fvpx was much more efficient at producing Vpx than pME18Neo-Fvpx upon transfection.

A series of mutants based on pEF-Fvpx were then constructed (Fig. 1a, c, e) and examined for their expression. First, we monitored the expression level of the 103/4A and 106/4A mutants to see if there is a significant difference that can account for the distinct growth phenotype of viruses carrying these mutations (Table 1). As shown in Fig. 1(c), only a faint amount of Vpx was detected for the 106/4A mutant and a deletion mutant lacking the entire PPM-coding region (d7P). Although considerably reduced relative to the WT clone, the 103/4A mutant clearly generated more Vpx than the 106/4A mutant. This result correlated well with the growth potentials of the WT, 103/4A, and 106/4A viruses (Table 1). Next, we determined the effect of the number and position of the alanine substitutions in PPM on Vpx expression (Fig. 1d). A single substitution of proline with alanine did not cause major reductions except for P106A (approximately 50 % of the WT level). Double and triple alanine substitutions gave distinct results. While the P104/2A, P103/3A and P105/3A mutations did not have a significant effect, the expression level of P107/3A relative to that of WT markedly decreased (similar to the P103/4A level). The P106/2A and P108/2A mutants expressed Vpx at a slightly reduced level as observed for P106A. The results in Fig. 1(c, d) showed that the number and position of consecutive prolines in PPM are important for Vpx expression. In addition to the PPM mutations, we analysed the mutational effect of the glycine-rich domain (GRD), which is a presumably flexible region just upstream of PPM (Fig. 1a). In general, poly-proline sequences form a rigid structure whereas glycine repeats provide flexibility. Therefore, we speculated that the GRD may affect the ability of PPM to enhance Vpx expression. However, the introduction of alanine substitutions into the GRD showed no appreciable effects (Fig. 1e).

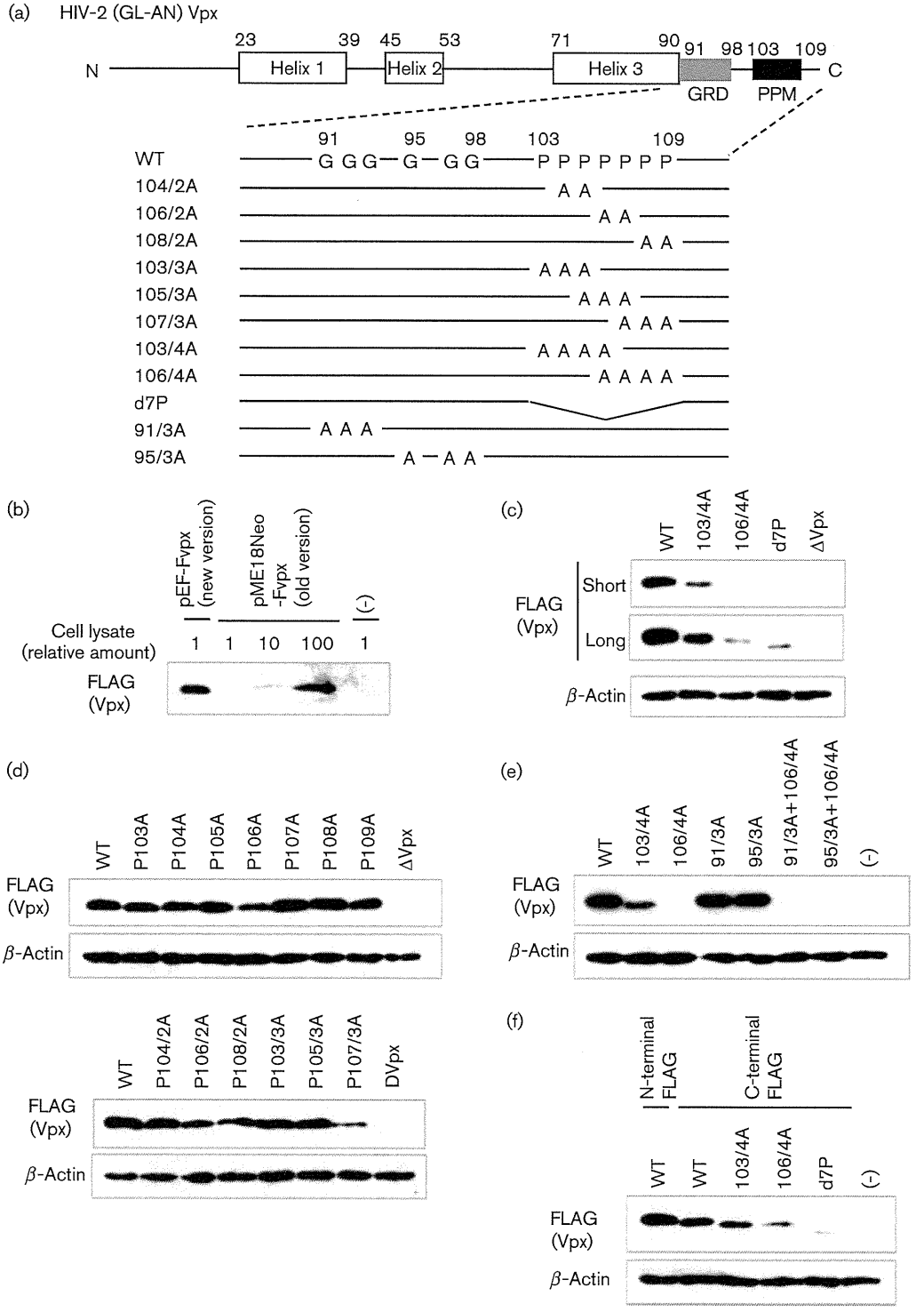

Fig. 1. Expression profiles of various Vpx–PPM mutants in transfected 293T cells. (a) A scheme of the domain structure and sequences of HIV-2 GL-AN Vpx (112 amino acids) and its mutants. Expression plasmids with N-terminal (pEF-Fvpx series)/C-terminal (pEF-vpxF series) FLAG were constructed in this study. Numbers indicate the positions of amino acid residues in the HIV-2 Vpx. GRD, glycine-rich domain; PPM, poly-proline motif. (b) Expression of Vpx from two expression plasmids designated pEF-Fvpx (this study) and pME18Neo-Fvpx (Fujita *et al.*, 2008a, b; Khamsri *et al.*, 2006). Relative amount of cell lysates used for Western blotting is indicated. (c) Expression of Vpx–PPM mutants carrying four successive alanine substitutions or a deletion. Short, short exposure; long, long exposure. (d) Expression of Vpx–PPM mutants carrying a single alanine substitution (upper) or two/three alanine substitutions (lower). (e) Expression of Vpx–GRD mutants with or without the 106/4A mutation. (f) Expression of Vpx–PPM mutants with a C-terminal FLAG tag. (-), pEF1/*myc*-HisA; WT, pEF-Fvpx or pEF-vpxF; ΔVpx, pEF-FxSt.

Table 1. Effect of mutations in HIV-2 GL-AN Vpx on its expression level and viral replication ability

Results obtained in 293T cells, lymphocytic HSC-F cells, and monocyte-derived macrophage (MDM) cultures (Fujita *et al.*, 2008a, b) are summarized.

Clone	Mutation*	Vpx expression†		Viral replication‡	
		Cells	Virions	HSC-F	MDM
GL-AN	None (WT)	WT	WT	WT	WT
GL-St	ΔVpx	UD	UD	ΔVpx	UD
GL-xP103A	P103A	WT	ND	WT	WT
GL-x103/4A	P103/4A	UD	UD	M	M
GL-x106/4A	P106/4A	UD	UD	ΔVpx	UD
GL-xP109A	P109A	WT	ND	WT	M

*ΔVpx, a frame-shift mutation in the *vpx* gene (Kawamura *et al.*, 1994); see Fig. 1 for P103A, P103/4A, P106/4A and P109A mutations.
†WT, wt level expression; UD, undetectable; ND, not done. Vpx proteins in transfected 293T cells (cells) and in virions prepared from transfected 293T cells (virions) were monitored. Vpx in cells was examined by using proviral clones and/or FLAG-tagged Vpx-expression vectors.
‡WT, similar replication to wt virus; ΔVpx, similar replication to GL-St virus; UD, undetectable; M, medium replication phenotype between WT and GL-St viruses.

Although our data here on the 103/4A and 106/4A mutants were consistent with the viral growth properties (Table 1), we asked whether there is a positional effect of the FLAG tag on the Vpx expression. Expression plasmids with a C-terminal FLAG tag based on pEF1/*myc*-HisA (pEF-vpxF constructs: WT, 103/4A, 106/4A and d7P) were constructed, and their ability to express Vpx upon transfection was analysed. As shown in Fig. 1(f), the data obtained were quite similar to those in N-terminal FLAG-tagged vectors. However, the difference in the expression level between clones appeared to be smaller (Fig. 1c, f). This might result from the adjacent effect of the C-terminal FLAG tag on PPM. We used N-terminal tagged versions (pEF-Fvpx clones) thereafter.

PPM facilitates translation of Vpx in a nucleotide sequence-independent manner

The results presented so far indicated that PPM is important for Vpx expression in cells. To further understand the mechanism underlying this observation, we compared the transcription and translation efficiencies of WT and PPM mutants (Fig. 2). We firstly measured mRNA levels in cells transfected with WT or three PPM mutants (103/4A, 106/4A and d7P). Total RNA was extracted from cells and relative *vpx* mRNA level was quantified by the real-time reverse-transcription-PCR (RT-PCR) method. As shown in Fig. 2(a), mutations in PPM did not significantly change the steady-state level of each mRNA in transfected cells. In agreement with this observation, the *in vitro* transcription assay gave similar results (Fig. 2a). However, when the Vpx proteins were synthesized by an *in vitro* transcription/translation system using rabbit reticulocyte lysates, the three PPM mutants were scarcely produced (Fig. 2b). In parallel with the data obtained in transfected cells, the amount of synthesized 103/4A was confirmed to be higher than that of 106/4A in independently repeated experiments (data not shown). Furthermore, we compared the translation efficiency of WT and 106/4A clones by an *in vitro* transcription/translation system using *Escherichia coli* S30 lysates. As seen in Fig. 2(b), the PPM mutation almost abrogated the translation of Vpx even in the bacterial system.

Then, we asked whether the effect of PPM on Vpx translation is linked to the unique secondary structure and/or poly-pyrimidine tract of mRNA around the PPM-coding region (Fig. 3a). At first, mutant plasmids carrying a stop codon just upstream of PPM (G102St and +103St) were constructed (Fig. 3a), and the expression of these mutant proteins was examined in transfected cells as well as in the cell-free system using rabbit reticulocyte lysates. The truncated mutants, G102St and +103St, migrated faster than WT Vpx and were expressed at a much lower level (Fig. 3b). This was also observed in the cell-free system (Fig. 3b). These results suggested that the amino acid sequences of PPM, but not the context of the RNA sequence, are essential for efficient translation of Vpx. Moreover, we constructed various clones with synonymous mutations (106/3ccg, 106/3cca, 105ccg, 106ccg, 107ccg and 104,106ccg) that potentially disrupt the poly-pyrimidine tract (Fig. 3a), and examined their expression levels in transfected cells and in the cell-free system. As shown in Fig. 3(c), the synonymous mutants were expressed as efficiently as WT Vpx. These data also indicated that the role of Vpx PPM is primarily determined by the context of the amino acid sequences, but not by that of nucleotide sequences. Taken together (Figs 2 and 3), our findings showed that the consecutive proline residues of PPM play an essential role in efficient translation of HIV-2 Vpx both in the eukaryotic and prokaryotic systems.

PPM of HIV-2 Vpx does not have a major effect on the expression level of HIV Vpr proteins

Vpx shares many properties with Vpr including virion-association, putative three-dimensional structure, and biological activities (Fujita *et al.*, 2010). However, no PPM is present in HIV-1 and HIV-2 Vpr proteins (Khamsri *et al.*, 2006). In addition, the stoichiometry of Vpx in the virion is much higher than that of Vpr (Singh *et al.*, 2000). Approximately 4000 Vpx are estimated to be packaged in one virion, while only 14–18 HIV-1 Vpr are encapsidated. In accordance with this observation, it has been previously reported that the expression level of HIV Vpr proteins in cells is low relative to that of HIV-2 Vpx as monitored by tagged

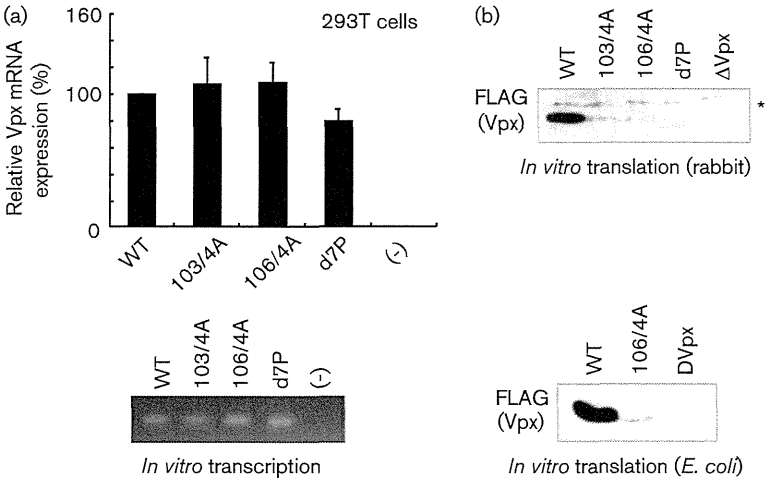

Fig. 2. Effect of PPM mutations on the expression of Vpx mRNA and protein. (a) Upper: relative amounts of Vpx mRNAs in transfected 293T cells. Total RNA was extracted from cells transfected with the expression plasmids indicated at 24 h post-transfection, and subjected to quantitative real-time RT-PCR analysis. Relative copy numbers are shown. (-), pEF1/*myc*-HisA. Lower: amounts of *in vitro* transcribed mRNAs for Vpx. (-), pEF1/*myc*-HisA. (b) Expression of Vpx–PPM mutants by an *in vitro* transcription/translation system using rabbit reticulocyte lysates (upper) or *E. coli* S30 lysates (lower). *, Non-specific bands; WT, pEF-Fvpx or pET-Fvpx; ΔVpx, pEF-FxSt or pET-FxSt.

expression plasmids/tagged proviral clones (Goujon *et al.*, 2008; Gramberg *et al.*, 2010; Khamsri *et al.*, 2006). Based on these results, we speculated that the addition of the HIV-2 Vpx PPM onto HIV-1/HIV-2 Vpr might enhance their expression.

We firstly compared expression levels of mRNA and protein for Vpx and Vpr. The mRNA levels for HIV-1 and HIV-2 Vpr proteins relative to that for HIV-2 Vpx in transiently transfected cells were measured by quantitative RT-PCR. As shown in Fig. 4(a), both Vpr mRNAs, HIV-1 Vpr in particular, were expressed to a lesser extent relative to Vpx mRNA. However, no major difference was noticed for Vpx and Vpr RNAs synthesized *in vitro* (Fig. 4a), probably due to T7 RNA polymerase in the reaction. When the protein expression levels were compared, more drastic results were obtained. HIV-1 and HIV-2 Vpr proteins were scarcely detectable in transfected cells and in the cell-free system (Fig. 4b), in contrast to Vpx. These results suggested that both transcription and translation processes are inefficient for Vpr expression. We then tested whether the PPM augments expression levels of HIV-1 and HIV-2 Vpr proteins by addition of the C-terminal flexible region of HIV-2 Vpx containing the PPM (Vpr1/Vpx and Vpr2/Vpx in Fig. 4c). In transfected cells, both Vpr1/Vpx and Vpr2/Vpx exhibited slightly higher expression relative to parental Vpr1 and Vpr2 clones, respectively (Fig. 4c). However, their expression levels obtained by adding the PPM were still much lower than that of Vpx. In addition, the *in vitro* transcription/translation analysis by rabbit reticulocyte lysates also gave little effect of the substitution with C-terminal flexible region on the translation efficiency (data not shown). These results showed that the addition of the Vpx PPM does not cause a major effect on the expression level of HIV Vpr proteins *in vivo* and *in vitro*.

SIVmac Vpx has PPM consisting of a hepta-proline stretch and its expression is PPM-dependent

For detailed analysis of Vpx and PPM-containing Vpr proteins, we generated a phylogenetic tree of various Vpx/Vpr proteins using SIVsyk (SIV from Sykes' monkeys) Vpr (without PPM) as a reference (Fig. 5). The Vpr of SIV from African green monkeys (SIVagm) has been suggested as an origin of Vpx (Sharp *et al.*, 1996). Notably, the Vpr of SIVagm clone GRI1677 has a PPM composed of five consecutive prolines, and its expression level is markedly reduced as a result of PPM-deletion (data not shown). The PPM (four consecutive prolines) of SIVmnd2 Vpx is located at a relatively similar position (106th to 109th proline) to our Vpx clone (HIV2 GL-AN in Fig. 5). Substitution mutations in this region (P106/4A) almost abolished Vpx expression (Fig. 1). Among various Vpr/Vpx proteins in Fig. 5, other than HIV-2 Vpx, Vpx proteins of SIV from drills (SIVdrl), SIVsmm and SIVmac have seven consecutive prolines.

Based on the results summarized above, we asked whether the P106/4A mutation in the Vpx–PPM of SIVmac gives an effect similar to that observed for HIV-2 Vpx (Fig. 1). As shown in Fig. 6(a), the sequence homology between the two proteins is quite high, the N-terminal half in particular, and the PPM is conserved as described above. Unexpectedly, the amount of SIVmac Vpx produced upon transfection was found to be significantly lower relative to that of HIV-2 Vpx (Fig. 6b). However, as clearly observed, the PPM mutant protein of SIVmac Vpx (106/4A) was expressed at a very reduced level relative to WT Vpx (Fig. 6b), indicating the presence of PPM-dependent regulation. We were interested in mapping the determinant(s) responsible for the different expression levels seen for HIV-2 and SIVmac Vpx proteins. Three chimeric expression plasmids were constructed, and monitored for their expression upon transfection (Fig. 6c). Since the three chimeric constructs expressed Vpx at a similarly low level to the WT SIVmac clone, the putative helix 1 in Vpx was considered to be the determinant. We substituted four amino acids in HIV-2 Vpx helix 1 with corresponding residues in the helix 1 of SIVmac Vpx (Fig. 6a, c). Expectedly, as is clear in Fig. 6(c), the mutant with the four substitutions (GL-D26N/I29V/A31E/L32I) and the WT SIVmac clone produced Vpx at a similarly low level upon